

## Pressurized Fast-Pyrolysis Characteristics of Typical Chinese Coals with Different Ranks

Chunyu Li,<sup>†,‡</sup> Jiantao Zhao,<sup>†</sup> Yitian Fang,<sup>\*,†</sup> and Yang Wang<sup>†</sup>

<sup>†</sup>Institute of Coal Chemistry, Chinese Academy of Sciences, Taiyuan 030001, People's Republic of China, and <sup>‡</sup>Graduate School of Chinese Academy of Sciences, Beijing 100039, People's Republic of China

Received May 11, 2009. Revised Manuscript Received September 9, 2009

The pressurized fast pyrolysis of three typical Chinese coals with different coal ranks (Huolinhe lignite, Shenmu bituminous coal, and Jincheng anthracite) was conducted on a self-made pressurized fixed-bed reactor. The physicochemical characteristics of the chars were studied via scanning electron microscopy (SEM), X-ray diffraction (XRD), and Fourier transform infrared spectroscopy (FT-IR). In addition, thermogravimetric analysis (TGA) at ambient pressure has been used to study the influence of the residence time, the pyrolysis temperature, and pressure on the gasification reactivity of residual chars. The results show that the change in char yield and reactivity with pressure, at a residence time of 1 min, is different from that at longer residence time. This is related to the changing impacts of the rapid primary release of volatiles and the slower secondary cracking reactions of the evolved tars and the graphitization of the char structure. Furthermore, as the coal rank, pyrolysis pressure, temperature, and residence time increase, the surface structure of the char becomes much denser, the degree of graphitization is enhanced, and the number of the functional groups is reduced, which lead to the decrease in the gasification reactivity of the coal char.

### 1. Introduction

Coal will still play an important role in the world's energy supplies with the projected levels of global economy. However, there has also been increasing environmental concern directed toward utilizing coal, for example, CO<sub>2</sub> emission, pollutant emissions, and particulate disposal.<sup>1</sup> Clean coal technologies are now being developed, because of their high efficiencies and minimal environmental impacts. Power generation using integrated gasification combined cycle (IGCC) and pressurized fluidized-bed combustion technologies, have attracted increased interest from the scientific and technological communities over the past decades. Pressurized coal gasification is not only the key part of the IGCC, but also the better approach to increase the gasification reaction rate and the capacity of the unit gasifier.<sup>2</sup>

Coal gasification is a very complex process; it consists of the devolatilization of coal particles (pyrolysis) and the gasification of residual char.<sup>3</sup> Pyrolysis is the primary and essential step of coal combustion and gasification. The treatment conditions in pyrolysis have a great effect on the yield and properties of residual char and, consequently, influence the coal gasification reactivity.<sup>4–6</sup> The pyrolysis and gasification

of coal are influenced by many factors, such as coal type, pressure, final temperature, residence time, etc.<sup>7–12</sup> Much of the fuel characterization data in the literature is based on thermogravimetric analysis (TGA), wire mesh, the fluidized-bed reactor, and entrained flow system. Sun et al.<sup>13</sup> studied the pyrolysis of two types of Chinese coal (with particle sizes of 0.4–4 mm) under pressure (1–13 atm) using a pressurized dual-chamber TGA instrument. Their results showed that, at higher temperature, the total yield decreases as the pressure increases, while the total weight loss is almost independent of pressure at low temperatures (<873 K). The bench-scale high-pressure fluidized-bed reactor system has been under research and development by Imperial College–London.<sup>14</sup> Their work showed that increases in either the temperature, pressure, or particle size had a negative impact on the char reactivity. Roberts et al.<sup>15</sup> determined that, although the apparent (as measured) reaction rate can be affected by pyrolysis pressure, the rate normalized to the char surface area (intrinsic rate) is much less affected, because of great effects of pyrolysis pressure on char micropore surface area. The pore

\*Author to whom correspondence should be addressed. Tel.: +86 351 2021137. E-mail address: fyf@sxic.ac.cn.

(1) Wall, T. F.; Liu, G. S.; Wu, H. W.; Roberts, D. G.; Benfell, K. E.; Gupta, S.; Lucas, J. A.; Harris, D. J. *Prog. Energy Combust. Sci.* **2002**, 28, 405–433.

(2) Huang, J. J.; Fang, Y. T.; Chen, H. S.; Wang, Y. *Energy Fuels* **2003**, 17, 1474–1479.

(3) Miura, K.; Nakagawa, H.; Nakai, S. I.; Kajitani, S. *Chem. Eng. Sci.* **2004**, 59, 5261–5268.

(4) Cloke, M.; Lester, E.; Gibb, W. *Fuel* **1997**, 76, 1257–1267.

(5) Jamil, K.; Hayashi, J. I.; Li, C. Z. *Fuel* **2004**, 83, 833–843.

(6) Alonso, M. J. G.; Borreg, A. G.; Alvarez, D.; Kalkreuth, W.; Menéndez, R. *Fuel* **2001**, 80, 1857–1870.

(7) Liu, H.; Kaneko, M.; Luo, C. H.; Kato, S.; Kojima, T. *Fuel* **2004**, 83, 1055–1061.

(8) Lemaignen, L.; Zhuo, Y.; Reed, G. P.; Dugwell, D. R.; Kandiyoti, R. *Fuel* **2002**, 81, 315–326.

(9) Griffin, T. P.; Howard, J. B.; Peters, W. A. *Fuel* **1994**, 73, 591–601.

(10) Harris, D. J.; Roberts, D. G.; Henderson, D. G. *Fuel* **2006**, 85, 134–142.

(11) Kajitani, S.; Suzuki, N.; Ashizawa, M.; Hara, S. *Fuel* **2006**, 85, 163–169.

(12) Chen, H. P.; Luo, Z. W.; Yang, H. P.; Ju, F. D.; Zhang, S. H. *Energy Fuels* **2008**, 22, 1136–1141.

(13) Sun, C. L.; Xiong, Y. Q.; Liu, Q. X.; Zhang, M. Y. *Fuel* **1997**, 76, 639–644.

(14) Cousins, A.; Paterson, N.; Dugwell, D. R.; Kandiyoti, R. *Energy Fuels* **2006**, 20, 2489–2497.

(15) Roberts, D. G.; Harris, D. J.; Wall, T. F. *Energy Fuels* **2003**, 17, 887–895.

structure of solid char varies greatly with the increasing pressure for different coal samples, and the gasification reactivity of residual chars decreases greatly as the pyrolysis pressure increases.<sup>12</sup>

Therefore, it is essential to investigate the influence of coal properties, the interaction between coal properties, and the operating conditions (such as the pyrolysis pressure, temperature, and the residence time) on coal pyrolysis and gasification. However, as the aforementioned equipments all have drawbacks (the reaction mechanism could not be analyzed on TGA, and the reaction time could not be exactly controlled on the wire mesh and the fluidized-bed reactor), these have rarely been systemically reported, especially the pyrolysis under longer residence time (> 5 min) at elevated pressures.

Therefore, it is urgent to establish advanced equipment to study these phenomena. In the present study, the pyrolysis behaviors of three types of Chinese coals with different ranks were investigated in a self-made pressurized fixed-bed reactor. The predominant feature of the equipment is that the sample can be easily moved and conveniently located by a magnet feeder under a specific pressure and temperature. Thus, the changes of the sample weight with the reaction time can be measured accurately. Furthermore, the physicochemical properties of the chars were studied and the gasification reactivity of residual chars was analyzed by an ambient thermogravimetric analyzer. Simultaneously, the influence of the coal rank on the behaviors of coal pyrolysis and char gasification was extensively analyzed.

## 2. Experimental Section

**2.1. Sample Preparation.** Three coal samples of different ranks were chosen for this study: Huolinhe lignite (HLH), Shenmu bituminous coal (SM), and Jincheng anthracite (JC). The original samples were ground and sieved to +80 mesh, i.e., the particle size is < 0.178 mm. The results of the proximate and ultimate analysis of coal samples are listed in Table 1. It can be observed that the volatile and oxygen contents of HLH coal are quite high, whereas the content of fixed carbon is very low; JC coal has the highest fixed carbon and ash contents, and it has the lowest volatile content.

**2.2. Experimental Apparatus and Method.** *2.2.1. Experimental Apparatus.* The pyrolysis experiments were performed in a pressurized fixed-bed reactor that is schematically shown in Figure 1. The fixed-bed reactor mainly consists of six parts: the pressure vessel, the furnace, the reactor, the temperature controller, the pressure adjustment system, and the sample transporter. The reactor is composed of a stainless steel tube with an inside diameter of 57 mm. A thermocouple is inserted in the middle of the reactor to measure and control the temperature. A quartz crucible is suspended at the bottom of the magnet. The diameter of the crucible is 30 mm, and the depth is 10 mm. The depth of the coal sample in the crucible is < 5 mm. The external diffusion effect has been tested and eliminated by increasing the gas velocity in the experiments.

*2.2.2. Experimental Method.* The pyrolysis procedure on the pressurized fixed-bed reactor is briefly elaborated as follows. The sample (2 g) is placed in a quartz crucible that is placed in upper chamber of the reactor. N<sub>2</sub> then is introduced into the reactor to displace the air and to increase the pressure to the desired value. The heaters are activated to increase the temperature to the required value. When the conditions are steady, the crucible is moved down to the heated zone using a magnetic force driving system. At the end of the test, the crucible is raised to the cold chamber. After depressurizing the reactor, the reacted sample is then moved out, weighed, and ground to 80 mesh for analysis and assessment of the gasification reactivity.

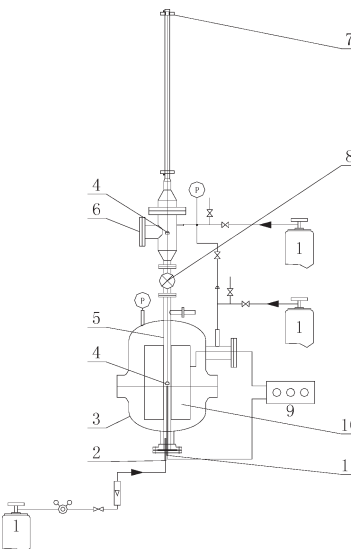


**Figure 1.** Schematic diagram of pressurized fixed-bed reactor. Legend: 1, N<sub>2</sub>; 2, gas inlet; 3, pressure vessel; 4, quartz crucible; 5, reaction pipe; 6, sampling entrance; 7, magnet; 8, ball valve; 9, temperature controller; 10, furnace; and 11, thermocouple.

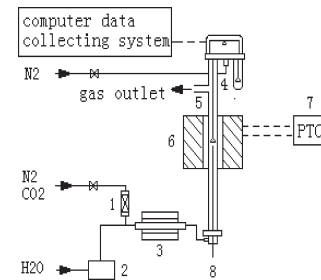


**Figure 2.** Schematic diagram of the thermobalance. Legend: 1, dryer; 2, water pump; 3, vaporizer and preheater; 4, TGS-2 thermogravimetric analyzer; 5, quartz reactor; 6, heater; 7, PTC-2 temperature controller; and 8, thermocouple.

Chars were prepared under a wide range of experimental conditions. Temperatures in the reactor were varied from 600 °C to 1000 °C (the heating rate in the pressurized fixed-bed reactor was calculated, and the value was likely to be > 1000 °C/s); the residence times and pressures that were investigated were 1–30 min and 0.1–0.7 MPa, respectively. Experiments were repeated 2–3 times under each condition. Reactivity values were averaged for each condition, and the standard deviations were < 10%.

The gasification experiments were conducted in a thermobalance (see Figure 2), which is comprised of an electrical furnace with an internal quartz tube reactor, a gas metering system, and a computer data collecting system. Initially, the sample is placed in the upper part of the reactor. The reactor then is heated in a N<sub>2</sub> atmosphere. When the temperature reaches the required value, the gasifying agent (H<sub>2</sub>O–N<sub>2</sub>) is introduced; the reactor is moved upward until the sample is located in the reaction zone. The conditions used are as follows: the sample weight is ~5 mg, the particle size is < 0.178 mm, and the gas flow rate is 100 mL/min. The reaction total pressure is 0.1 MPa, and the steam fraction in the feed gas is 60% (in volume). The reaction temperature is 950 °C.

The half-weight loss rate ( $R_{50}$ ) in the rectilinear region was taken (from the recorded weight-time curve) as the gasification reactivity of the char.

*2.2.3. Physicochemical Analysis of Char.* The superficial morphologies of chars were examined by scanning electron

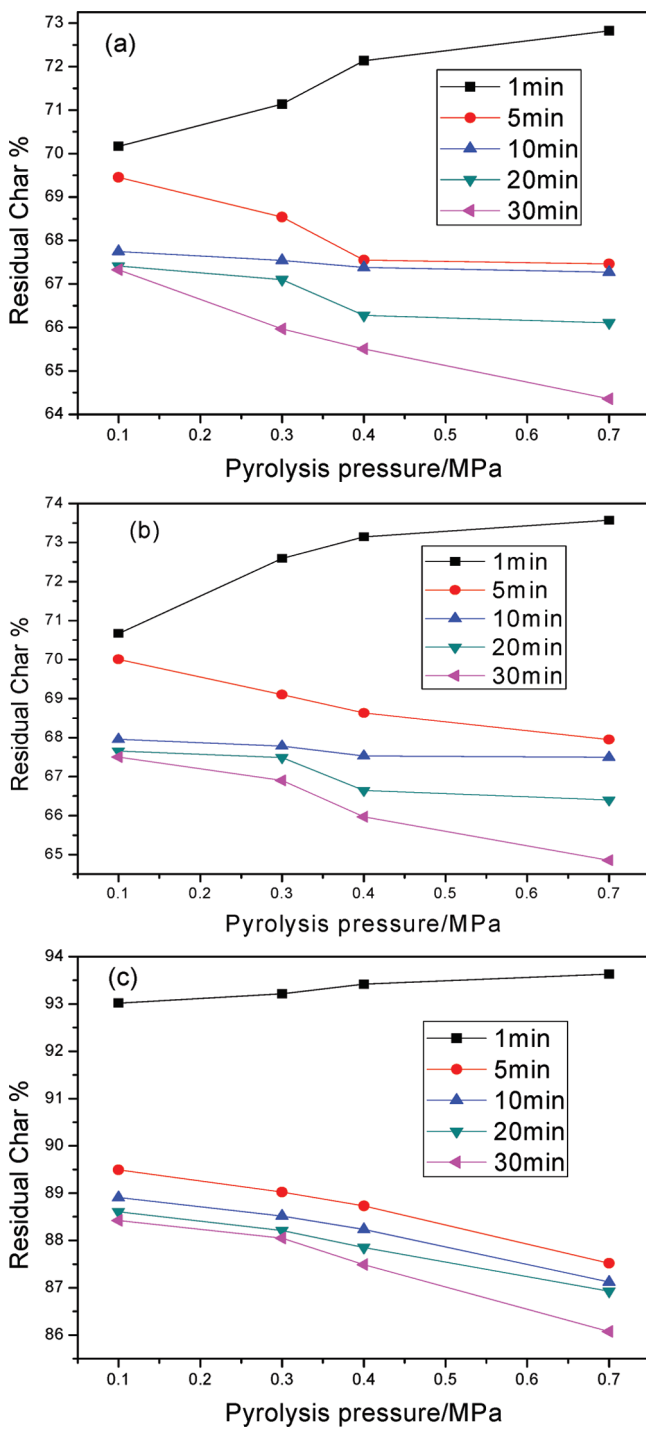


**Figure 3.** Effect of residence time and pyrolysis pressure on the product yields at 900 °C for various coals: (a) HLH, (b) SM, and (c) JC.

microscopy (SEM), the samples were observed under an acceleration voltage of 15 kV. X-ray diffraction (XRD) patterns were measured on a Bruker Advanced X-ray Solutions/D8-Advance using Cu K $\alpha$  radiation; the anode was operated at 40 kV and 40 mA. The Scherrer formula was used to calculate the structure parameters of stacking height ( $L_C$ ) and radial spread ( $L_A$ ). To ensure the reliability of  $L_A$  and  $L_C$ , we repeated the pyrolysis experiment 2–3 times under each condition and performed the corresponding XRD measurement. In addition, the data of  $L_A$  and  $L_C$  were averaged for each condition. FT-IR spectra were recorded on a Nicolet Magna 550 instrument with a DTGS KBr detector.

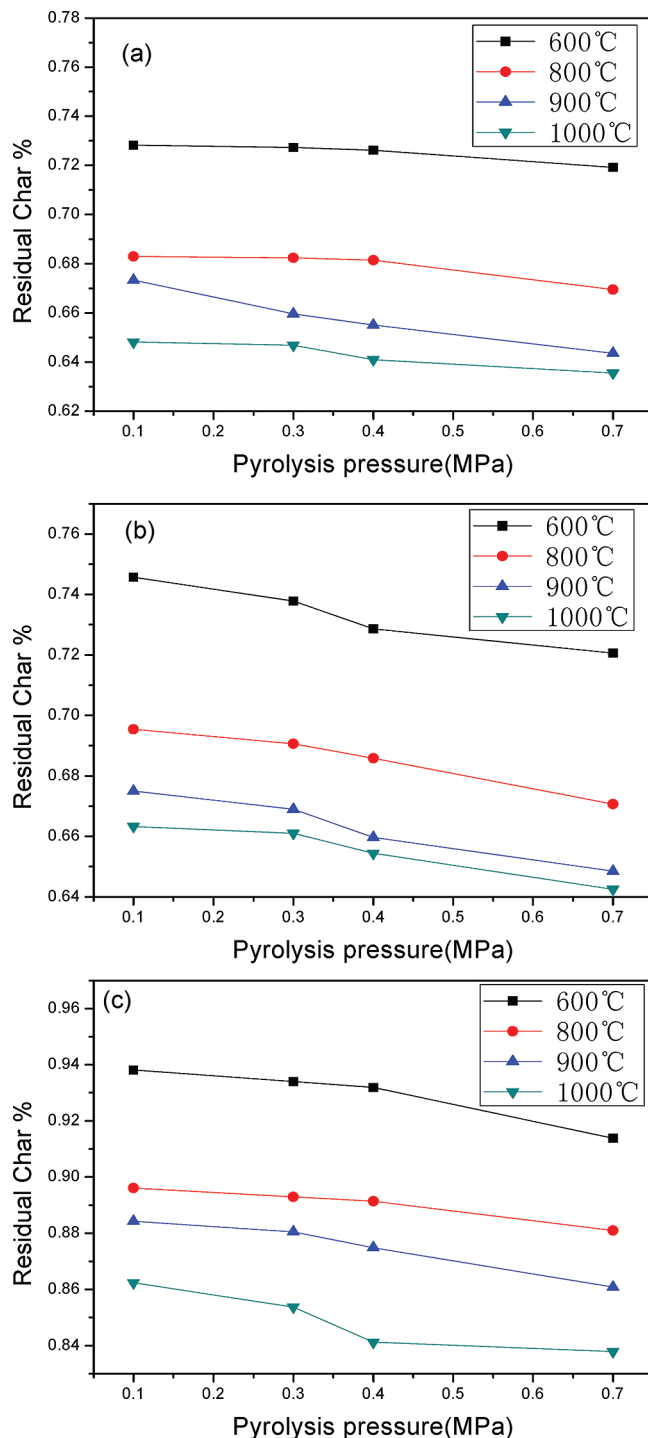


**Figure 4.** Effect of temperature and pyrolysis pressure on the product yields at a residence time of 30 min for various coals: (a) HLH, (b) SM, and (c) JC.

### 3. Results and Discussion

**3.1. Pyrolysis of Coal Particle Size.** The pyrolysis of three types of coals with different rank was performed at pressures of 0.1–0.7 MPa, residence times of 1–30 min, and temperatures of 600–900 °C. As shown in Figure 3, the char yield at a residence time of 1 min is consistent with the previous findings.<sup>12–16</sup> However, it is different from that at longer

(16) Bautista, J. R.; Russel, W. B.; Saville, D. A. *Ind. Eng. Chem. Fundam.* **1986**, 25, 536–544.

**Table 1. Proximate and Ultimate Analyses of Three Coal Samples**

sample	Proximate Analysis (wt %,ad)			Ultimate Analysis (wt %,ad)				
	V	M	A	C	H	O	N	St
HLH	26.30	10.24	35.56	38.80	2.23	12.07	0.82	0.28
SM	27.53	7.12	12.56	63.36	4.15	11.49	0.95	0.37
JC	7.44	0.89	23.52	66.93	2.63	3.68	0.82	1.53

residence times. At a residence time of 1 min, the char yield increased as the pressure increased, which is in good agreement with the report of Bautista et al.,<sup>16</sup> in which the weight loss of Pittsburgh coal decreased rapidly as the pressures of helium and hydrogen increased to an apparent limiting value at 10 atm. At longer residence times (such as 5–30 min), however, the char yield decreases as the pressure and residence time each increase. Generally, the pyrolysis includes two processes: (i) the removal of moisture and the breakage of weak bonds and (ii) the secondary pyrolysis of the condensed carbon matrix. The trends observed suggest that there is a competition between the two opposing effects with increasing pressure. It is generally agreed that the effects of pressure on the pyrolysis are as follows: (1) the pressure inhibits the release of tar and volatiles; (2) the pressure enhancements in the heat- and mass-transfer rates result in the acceleration of the second reaction of the large molecules in the coal volatiles, causing the weight loss. At shorter residence times (1 min, for example), the weak bonds in the original coal sample begin to break, and gases that form are evolved. It seems that the inhibiting effect of the pressure is dominant and the increased char yield with the increasing pressure is due to the suppression of tar and volatiles release by the physical effect of pressure. At longer residence times (5–30 min), however, the increased rate of the secondary reaction at higher pressures become dominant.<sup>17</sup> This implies that, at longer residence times, the higher pressures increase the density of material trapped within the particles. It also increases the heat-transfer rate, which leads to an increased rate of cracking of the large organic groups. The secondary decomposition is enhanced as the pressure increases the residence time of the volatile product inside the particles. This promotes cracking and leads to more gas being released and reduces char yields.<sup>18</sup> Thus, the secondary reaction is accelerated, resulting in the decrease in char yield.

The char yields for the three coals at different pyrolysis temperatures and pressures and a certain residence time are shown in Figure 4. It is observed that the residual chars decrease as the temperature increases, which is especially noticeable at temperatures of 600–800 °C. That may be explained as follows:

(1) The decisive role of the pyrolysis temperature. That is because the pyrolysis temperature governs the reaction path of the coal pyrolysis reaction and decides the yields of the product.<sup>19</sup>

(2) The higher pyrolysis temperature enhances the release rate of the volatile matters and decreases the residence time of it in the interior of the particle, which decreases the chance of the condensation reaction and the secondary reaction.<sup>20</sup>

(17) Solomon, P. R.; Serio, M. A.; Carangelo, R. M.; Markham, J. R. *Fuel* 1986, 65, 182–194.

(18) Yang, H. P.; Chen, H. P.; Ju, F. D.; Yan, R.; Zhang, S. H. *Energy Fuels* 2007, 21, 3165–3170.

(19) Wang, P.; Bu, X. P.; Xin, S. H.; Deng, Y. Y. *Coal Chem. Ind.* 2005, 2, 20–23.

(20) Mermoud, F.; Salvador, S.; Steene, L. V. D.; Golfier, F. *Fuel* 2006, 85, 1473–1482.

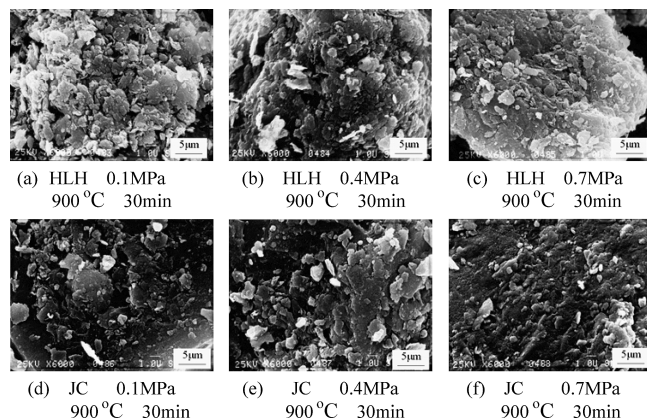


Figure 5. SEM photomicrographs of the chars.

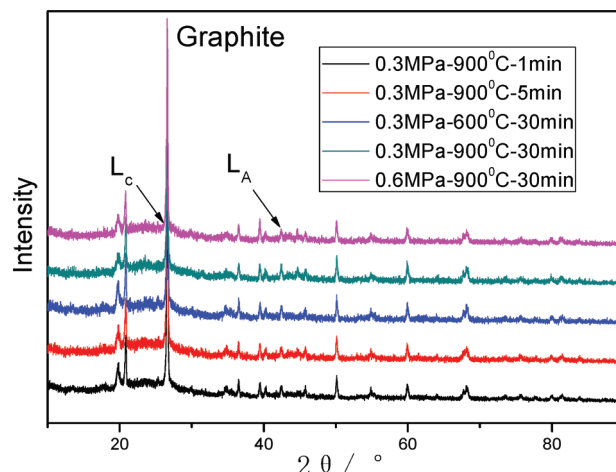


Figure 6. XRD patterns of the chars from HLH pyrolysis under different conditions.

Thus, the increase of the pyrolysis temperature enhances the pyrolysis reaction of coals and decreases the chars yield.

Figure 4 also shows that the quantity of char decreases as the pressure increases. This has been observed in previous work and is explained by the effect of the heat-transfer rate.<sup>12–14</sup>

The char yields of the three coals—the JC coal, the SM coal, and the HLH coal—under the same pyrolysis conditions can also be compared, as shown in Figures 3 and 4. It can be seen that, as the coal rank increases, the char yields increase, which may be related to the difference of the coal structure. As is generally realized, the thermal stability of the aromatic ring is much greater than that of the side-chain and active sites. In the low-rank coal, there are more side-chain and active sites, which are easy to decompose at high temperature. In addition, the different volatile contents in the three types of coal will also contribute to the variation in the char yields. As it can be seen from the elemental analysis (recall Table 1), the volatiles contents are 7.44%, 27.53%, and 26.30% for the JC coal, SM coal, and HLH coal, respectively.

**3.2. Physicochemical Characteristics of Solid Char.** The SEM observation of the residual chars prepared under different conditions was performed. Figure 5 shows the SEM images of the HLH char and the JC char prepared under 0.1, 0.4, and 0.7 MPa at a residence time of 30 min and a reaction temperature of 900 °C. With the increase of

Table 2. Crystallite Dimensions of the Carbon in the Chars

sample	HLH (MPa·°C·min)				0.3–900–30	SM (MPa·°C·min)	JC (MPa·°C·min)
	0.3–900–1	0.3–900–5	0.3–600–30	0.6–900–30			
$L_c$ (nm)	1.279	1.334	1.211	1.457	1.385	1.715	2.067
$L_a$ (nm)	2.336	2.307	2.324	2.492	2.464	2.581	3.633

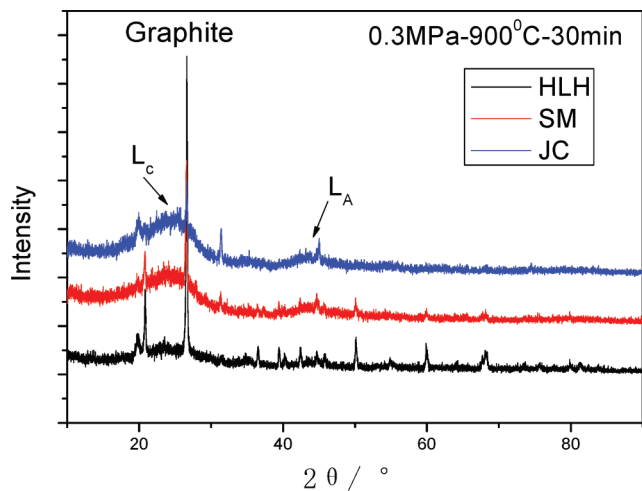


**Figure 7.** XRD patterns of the chars from the pyrolysis of three coals under the same conditions.

pressure, the surface morphology of chars obtained from the HLH and JC coal shows similar changes. The char obtained at 0.1 MPa is really the residue formed after volatile matters are emitted and the surface of the tested char proves to be irregular. The solid carbon particles look like balloons, which means that the coal particles have melted and swelled by emitting volatiles during pyrolysis.<sup>21</sup> With the increase of pressure, the surface of the tested char becomes smooth. High pressure results in the ordering of carbon layers and an increase in the degree of graphitization. The surface structure of residual char is dense and plugged by volatile matters, which indicates that the surface might have become less reactive to gasification.<sup>14,22</sup> Comparing the chars obtained from the two types of coal, the main difference is that the surface of the JC char is smoother and blacker than that of HLH char, which is probably related to the difference in the ranks of the parent coals.

XRD provides information regarding the extent of char crystallinity. The XRD patterns for chars obtained from HLH char (coal or char) are presented in Figure 6. The chars made in the reactor at various residence times, temperatures, and pressures are first considered. Each spectrum has a strong, narrow signal at  $26.6^\circ 2\theta$ , which is from the single-crystal  $\text{SiO}_2$  sample holder. The major peak is centered at  $\sim 25^\circ 2\theta$ , which corresponds to the  $L_c$  (stacking height) of the crystal lattice. The minor band centered at  $\sim 44^\circ 2\theta$  is associated with the  $L_a$  (radial spread) dimension.<sup>15</sup> With the increase of the residence time, temperature, and pressure, the intensities of  $L_a$  and  $L_c$  become stronger, which indicates that the lattice structure of char is better and the degrees of graphitization become higher (see Table 2).

Figure 7 shows the XRD spectra for chars obtained from JC coal, SM coal, and HLH coal under the same pyrolysis

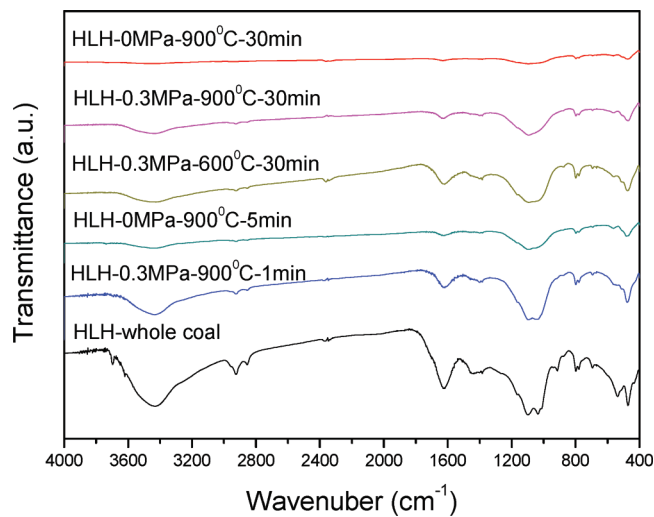


**Figure 8.** FT-IR spectra of the chars from HLH coal pyrolysis under different conditions.

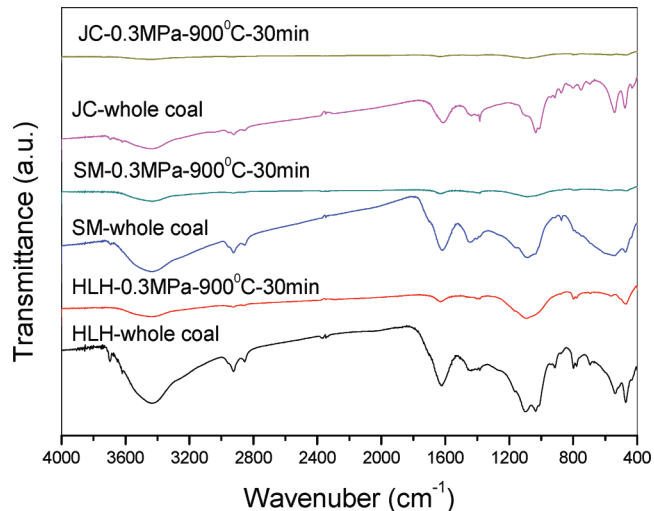


**Figure 9.** FT-IR spectra of the chars from the pyrolysis of three coals under the same conditions.

conditions. All of the chars show similar diffraction peaks at  $2\theta = 25^\circ$  and  $44^\circ$ , respectively. This suggests consistency in the main crystal structures of the chars as the pyrolysis pressure changed. The diffraction peak intensity of the char made from JC coal is the strongest, that from SM coal is the second strongest, and that from HLH coal is the weakest. This results show that the higher coal rank, the stronger the intensity of  $L_a$  and  $L_c$  (see Table 2).

Figure 8 presents FT-IR spectra of the char from HLH coal prepared at various residence times, temperatures, and pressures. Marked decreases with increasing residence time, temperature, and pyrolysis pressure are observed in the intensities of both the aliphatic C–H stretching transmittance bands ( $3000\text{--}2920\text{ cm}^{-1}$ ,  $1450\text{ cm}^{-1}$ ) and of the hydrogen-bonded –OH transmittance band ( $\sim 3400\text{ cm}^{-1}$ ).

(21) Miura, K.; Nakagawa, H.; Nakai, S. I.; Kajitani, S. *Chem. Eng. Sci.* **2004**, *59*, 5261–5268.

(22) Cai, H. Y.; Guell, A. J.; Chatzakis, I. N.; Lim, J. Y.; Dugwell, D. R.; Kandiyoti, R. *Fuel* **1996**, *75*, 15–24.

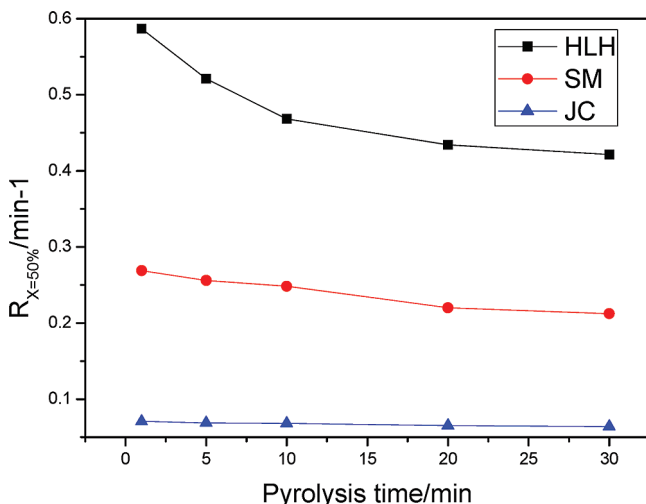


**Figure 10.** Gasification reaction rates of the chars pyrolyzed at different residence times (0.3 MPa and 900 °C).

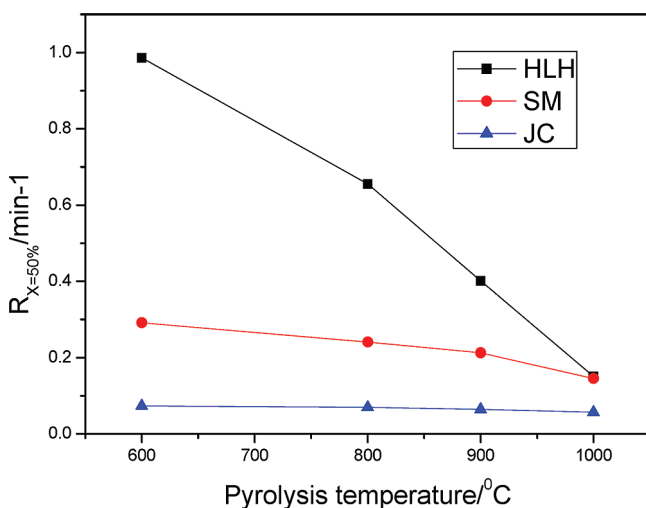


**Figure 11.** Gasification reaction rates of the chars pyrolyzed at different temperatures (0.3 MPa, 30 min residence time).

The 1600  $\text{cm}^{-1}$  band was also observed to decrease as the pyrolysis residence time, temperature, and pressure each increased. Because the intensity of this band is believed to be enhanced in the presence of a polar substituent on the aromatic rings (such as  $-\text{OH}$ ), the decrease, coupled with the decrease of the 3400  $\text{cm}^{-1}$  band suggests the disappearance of phenolic  $-\text{OH}$  groups from aromatic structures in the chars.<sup>22</sup> This phenomenon implies that increases in the pyrolysis residence time, temperature, and pressure can accelerate the decomposition of the phenolic  $-\text{OH}$ .

Figure 9 shows the changes in FT-IR spectra of the three coals and chars derived under the same pyrolysis conditions. The three coals have remarkably similar FT-IR spectra. However, as the coal rank increases, the intensity of the  $-\text{OH}$  stretching vibration of the char decreases and that of the aromatic ring increases. The  $-\text{OH}$  mainly exists in the terminal group and side chain; it is active and can be easily condensed to  $\text{H}_2\text{O}$  during the pyrolysis reaction. In the coal, the  $-\text{OH}$  exists in the polymeric structure, which would facilitate the formation of hydrogen bonds. With the increase of the coal rank, the  $-\text{OH}$  population of the polymeric structure decreases. Thus, the contribution of the hydrogen

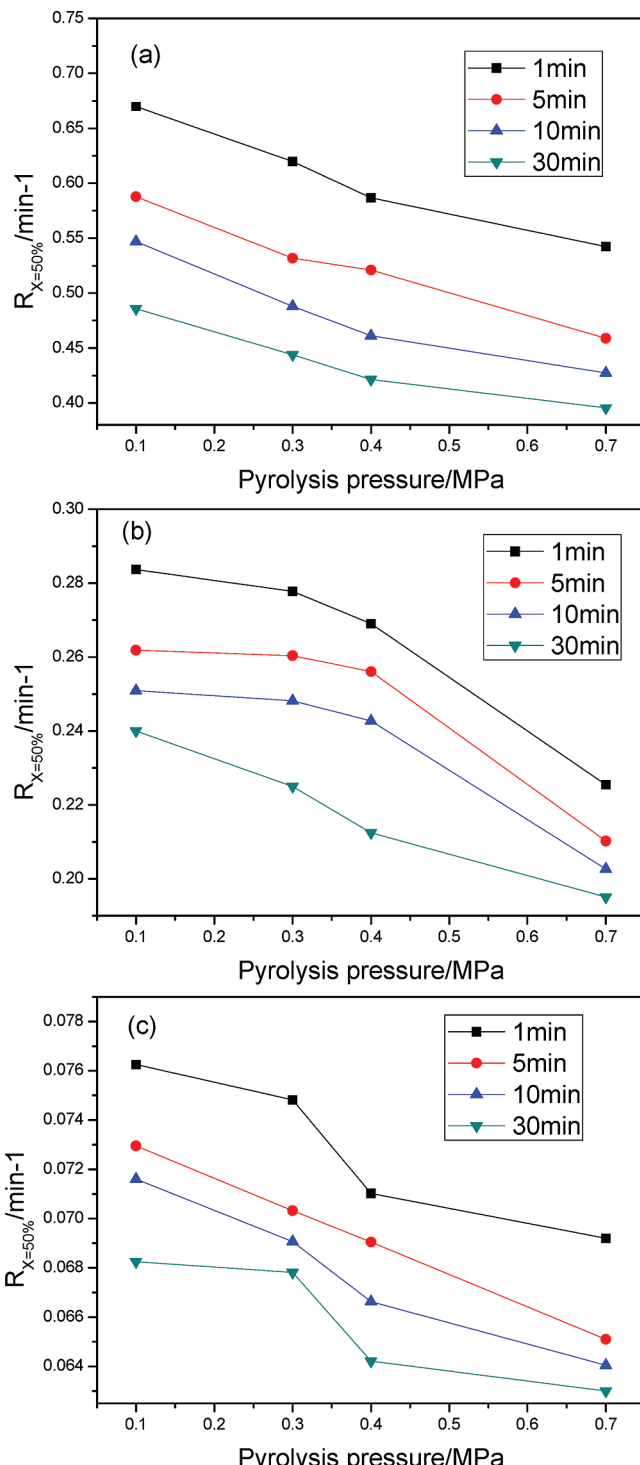


**Figure 12.** Gasification reaction rates of the chars pyrolyzed at different pressures with 900 °C for various coals: (a) HLH, (b) SM, and (c) JC.

bond to the coal reactivity in the high rank coal would also be weakened.<sup>23</sup>

**3.3. Characteristics of Char Gasification.** The isothermal gasification behavior of the resultant char was investigated in an ambient pressure thermal analyzer with steam as the gasifying agent; the weight loss graphs are plotted in Figures 10 and 11. The char obtained from the lower-rank HLH coal is more

(23) Feng, J.; Li, W. Y.; Xie, K. C. *J. China Univ. Min. Technol. (Chin. Ed.)* 2002, 31, 362–366.

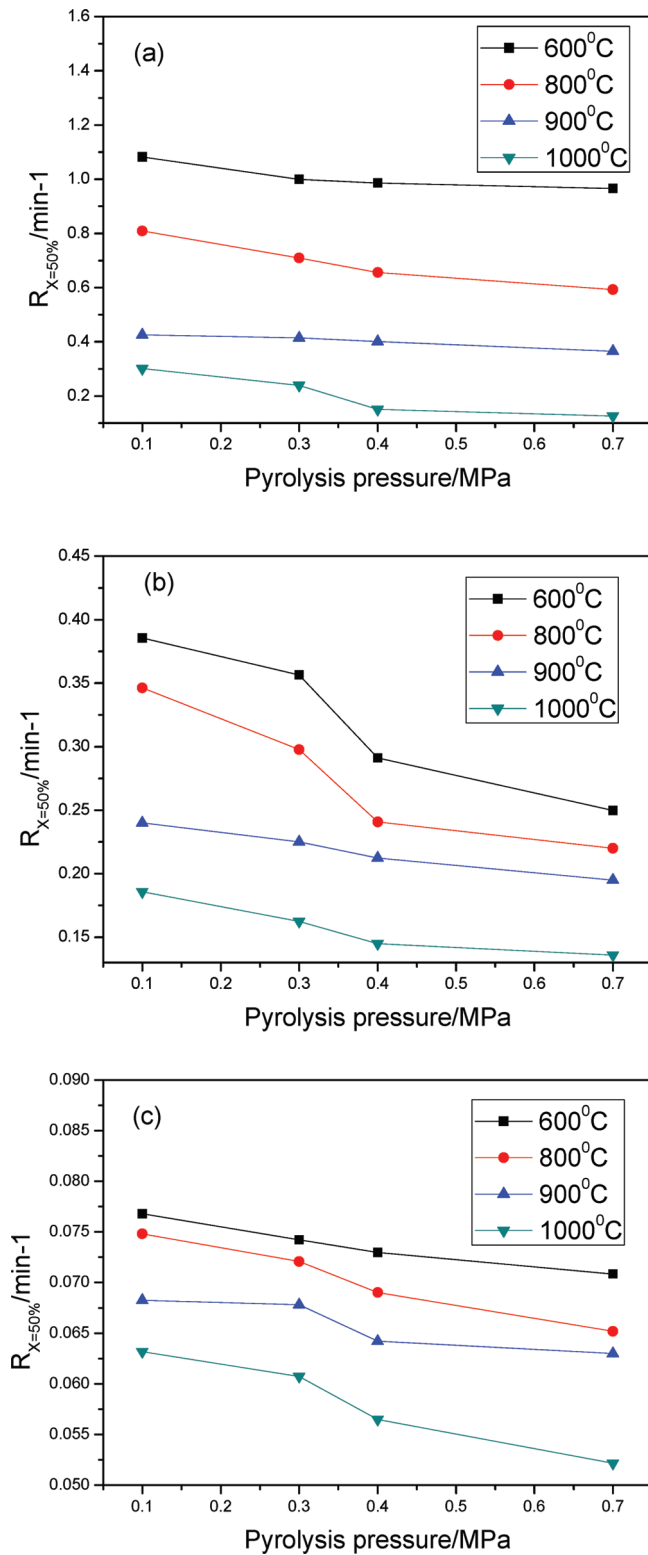


**Figure 13.** Gasification reaction rates of the chars pyrolyzed at different pressures with a residence time of 30 min for various coals: (a) HLH, (b) SM, and (c) JC.

reactive than those from the SM and JC coals. All the samples are determined to exhibit a qualitatively similar behavior, showing marked reductions in char reactivity with increasing residence time and temperature at the pressure of 0.3 MPa. It is generally believed that the reactivity of the char is related to the degree of graphitization of the char. The SEM, XRD, and

FT-IR results indicate that, with the increase of residence time and temperature, the population of the organic function groups decreases and the degree of graphitization increases. Thus, the decrease of reactivity of char is due to the increase in the degree of graphitization. Figures 10 and 11 also show that the decrease in reactivity is observed to be greater for the HLH char; this may be due to the faster diminishing rate of the organic function groups for the HLH char, which leads to the increase in the degree of graphitization.

Pyrolysis char samples have been prepared under pressures in the range of 0.1–0.7 MPa. Figures 12 and 13 present the gasification reactivities of these pyrolysis chars prepared from the HLH, SM, and JC coals, as a function of pressure. The reactivities of all three chars decrease as the pyrolysis pressure increases, which is consistent with the studies of Hanping Chen.<sup>12</sup> According to their research, the increased fluidity that resulted from higher-pressure pyrolysis leads to an enhanced ordering of carbon layers and a subsequent loss of gasification reactivity of the char residue.<sup>24</sup> Therefore, combined with the XRD, SEM, and FT-IR results in the present work, the decrease of the reactivity of the char is thought to be due to the increase in the degree of graphitization as the pressure increases. Temperature, pressure, and particle size have an impact on this process. The char reactivity decreases rapidly with the pyrolysis of the coal. This is thought to have resulted from the rapid decomposition of secondary, unreactive char within the pores of the material. Over a longer time scale, the structural is reorganized in the solid char, which causes the graphitization of char.<sup>14</sup>

#### 4. Conclusion

The influence of pressure, temperature, and residence time on coal pyrolysis, physicochemical characteristics, and gasification reactivity of resultant coal chars was investigated systematically. The main conclusion can be summarized as follows:

(1) With increasing pyrolysis pressure, the char yield at the residence time of 1 min is increased, but it decreases at residence times of 5–30 min. At a residence time of 1 min, the inhibiting effect of the pressure is dominant and, thus, the char yield increases as the pressure increases. At longer residence times, the breaking of large organic functional groups and the secondary reaction is accelerated by pressure which results in a reduction of the char yield. The char yields decrease as the pyrolysis temperature and the residence time each increase.

(2) The surface structure of the char becomes much denser, the graphitization degree is enhanced, and the number of the functional groups is reduced as the pyrolysis pressure, temperature, and residence time each increase.

(3) The increases in pressure, temperature, and residence time, as well as the coal rank during pyrolysis, decreases the char gasification reactivity, which may be due to the decrease in the number of organic functional groups and the increase in the degree of graphitization.

**Acknowledgment.** This work was supported by the Major State Basic Research Development Program of China (973 Program, No. 2006JQJ11131), the National High-Tech R&D Program of China (863 Program, No. 2007AA050302), and Knowledge Innovation Program of the Chinese Academy of Sciences (KGCX2-YW-320).

(24) Lee, C. W.; Jenkins, R. G.; Schobert, H. H. *Energy Fuels* 1992, 6, 40–47.